

## THEORETICAL STUDY OF A FLEXIBLE WIRETYPE JOULE THOMSON MICRO-REFRIGERATOR FOR USE IN CRYOSURGERY

**Adhika Widyaparaga**

Department of Mechanical Eng., Kyushu University  
Fukuoka, Japan

**Masashi Kuwamoto**

Department of Mechanical Eng., Kyushu University  
Fukuoka, Japan

**Naoya Sakoda**

International Research Center for  
Hydrogen Energy, Kyushu  
University  
Fukuoka, Japan

**Masamichi Kohno**

Department of Mechanical Eng.,  
Kyushu University  
Fukuoka, Japan

**Yasuyuki Takata**

Department of Mechanical Eng.,  
Kyushu University  
Fukuoka, Japan

### ABSTRACT

We have developed a model capable of predicting the performance characteristics of a wiretype Joule-Thomson microcooler intended for use within a cryosurgical probe. Our objective was to be able to predict evaporator temperature, temperature distribution and cooling power using only inlet gas properties as input variables. To achieve this, the model incorporated changing gas properties due to heat transfer within the heat exchanger and isenthalpic expansion within the capillary. In consideration of inefficiencies, heat in-leak from free convection and radiation was also considered and the use of a 2D axisymmetric finite difference code allowed simulation of axial conduction. Two types of microcoolers differing in inner tube material, poly-ether-ether-ketone (PEEK) and stainless steel, were tested and simulated. CO<sub>2</sub> was used as the coolant gas in the calculations and experimental trials for inlet pressures from 0.5 MPa to 2.0 MPa. Heat load trials of up to 550 mW along with unloaded trials were conducted. Comparisons to experiments show that the model was successfully able to obtain a good degree of accuracy. For the all PEEK microcooler in a vacuum using 2.0 MPa inlet pressure,

the calculations predicted a temperature drop of 57 K and mass flow rate of 19.5 mg/s compared to measured values of 63 K and 19.4 mg/s therefore showing that conventional macroscale correlations can hold well for turbulent microscale flow and heat transfer as long as the validity of the assumptions is verified.

### INTRODUCTION

Cryosurgery is a surgical method which involves freezing undesirable tissue such as cancerous tumors with the objective to destroy that particular tissue. The structure of cells and their naturally surrounding medium allow a certain resistance towards freezing. As described by Mazur [1], down to 268 K, the dissolved salts within intracellular water reduce the freezing point. The plasma membrane can inhibit growth of ice crystals into the cytoplasm further preventing cell contents from freezing. Therefore to obtain freezing as such required in cryosurgery, the cell temperature must be reduced to a lower level. An early study by Cooper[2] established that 253 K is sufficient to cause tissue necrosis and several studies observed the lethal temperature threshold to be 258 K[3, 4]. However,

Gage and Baust [5] state that at these temperatures there is still a degree of uncertainty regarding cell destruction and recommend temperatures between 233 to 223 K to be the critical temperature in which cell death occurs.

It is a common practice to apply freeze/thaw cycles in cryosurgery as the cell death count is also dependent on the freezing rate and, even more so, the thaw rate. Thawing promotes the growth of larger intracellular ice crystals due to recrystallization and aggregation of smaller crystals formed during initial freezing. A high cooling rate is important as it will determine the degree to which intracellular ice is formed [1]. Gage et al [6] conducted a study evaluating the effect of cooling rates and thawing rates on cell necrosis. The study set the rapid cooling rate at 30 K per minute. The cell death rate was found to be highest when the tissue is first rapidly cooled, held at the temperature for 4 minutes and then thawed slowly. The best results were obtained when the cells were held at 237 K to 223 K. Rapid cooling is one of the merits of the Joule-Thomson cooler and therefore it is very suitable for cryosurgery purposes.

Several studies have been conducted in regards to theoretical calculation of Joule-Thomson cooler performance. Lerou et al [7] used the entropy generation minimization method for dimensional optimization of the counterflow heat exchanger for a microfabricated Joule-Thomson microcooler design. They set predetermined temperatures of 96 K and 300 K as the minimum and maximum temperatures respectively. Derking et al [8] focused on optimization of the operating gas. However, both studies did not simulate the isenthalpic expansion process. Studies simulating the isenthalpic expansion process of Joule-Thomson cooling include work by Chou et al [9] and improved upon by Maytal [10], yet these studies did not involve the incorporation of a heat exchanger to model a complete Joule-Thomson cooler. The most complete study that we have encountered so far regarding the modeling of both the heat exchanger and the isenthalpic expansion of a Joule-Thomson cooler is the numerical study by Ng et al [11]. They used the modified Benedict-Webb-Rubin equations of state for Argon to predict temperature profiles of a Joule-Thomson cooler. Five boundary conditions consisting of the flow rate and inlet and outlet temperatures and pressures of the two ends of the heat exchanger are to be inputted and a prediction of the temperature distribution will be calculated. Therefore, based on these previous studies, it seems that there has been no attempt to predict the performance and temperature distribution of a Joule-Thomson cooler based on only the input of inlet gas temperature and pressure at the entrance of the microcooler. Since the required inlet gas properties and its relation to cooler performance is of importance to the user of these devices, it is thus necessary to be able to predict the end performance for any given inlet gas pressure, temperature and gas species without reliance on any other working gas related inputs.

We have manufactured two types of concentric wiretype Joule-Thomson microcoolers of different inner tube material.

Microcooler A uses an inner tube constructed of SUS 304 stainless steel ( $k = 16 \text{ W K}^{-1} \text{ m}^{-1}$ ) while microcooler type B uses poly-ether-ether-ketone ( $k = 0.25 \text{ K}^{-1} \text{ m}^{-1}$ ). Both microcoolers consist of an outer tube constructed from PEEK. This study intends to simulate the function of the wire-type Joule Thomson microcooler using a 2D axisymmetric finite difference code and predict the evaporator temperature using only the inlet gas pressure and temperature as input variables. This involves the combined calculation of the heat transfer within the heat exchanger and the Joule-Thomson expansion process.

## NOMENCLATURE

$f$	friction factor
$h$	enthalpy ( $\text{J kg}^{-1}$ )
$L$	characteristic length (m)
$\dot{m}$	mass flow rate ( $\text{kg s}^{-1}$ )
$Q$	heat flow rate (W)
$T$	Temperature (K)

## Dimensionless groups

$Pr$	Prandtl number
$Nu$	Nusselt number
$Re$	Reynolds number
$Ra$	Rayleigh number
$Kn$	Knudsen number

## Greek symbols

$\rho$	mass density ( $\text{kg m}^{-3}$ )
$\lambda$	free mean path (m)
$\mu_{JT}$	Joule Thomson coefficient ( $\text{K Pa}^{-1}$ )

## Subscripts

$in$	inlet
$out$	outlet
$n$	horizontal element number
$m$	vertical element number
$i$	iteration count
$h$	hot section
$c$	cold section
$e$	environment
$rad$	radiation

## DEVICE DESCRIPTION

The main operative components of the Joule Thomson microcooler are the capillary and the heat exchanger. The primary cooling process is the isenthalpic expansion which occurs in the capillary. The capillary has a length of 50 mm and a nominal inner diameter of 100  $\mu\text{m}$ .

The capillaries we used were from two different manufacturers. We will refer to these as capillary A and capillary B. We used capillary A for our earlier work with the stainless steel inner tube microcoolers (Microcooler A) while our later work (Microcooler B) used capillary B. It is important

to mention this since the manufacturing quality between both capillaries differs. For both products, the nominal value of the capillary inner diameter from both manufacturers is officially stated as 100  $\mu\text{m}$  with a deviation of up to 20%. The large deviation makes it imperative that we determine the actual inner diameter.

Four samples were taken from each capillary type and observed under Scanning Electron Microscopy (SEM). Figures 1a and 1b show capillaries A and B respectively. The results revealed actual diameters of capillaries A and B to have an average of 114.5  $\mu\text{m}$  and 100.1  $\mu\text{m}$  respectively. The 450 mm long heat exchanger consists of a poly-ether-ether-ketone (PEEK) outer tube with an inner diameter of 0.6 mm and wall thickness of 0.2 mm. The outer tube was arranged concentrically with a SUS304 austenitic stainless steel inner tube for Microcooler A or a PEEK inner tube for Microcooler B. The inner tube was of 0.4 mm outer diameter and had 0.1 mm wall thickness.

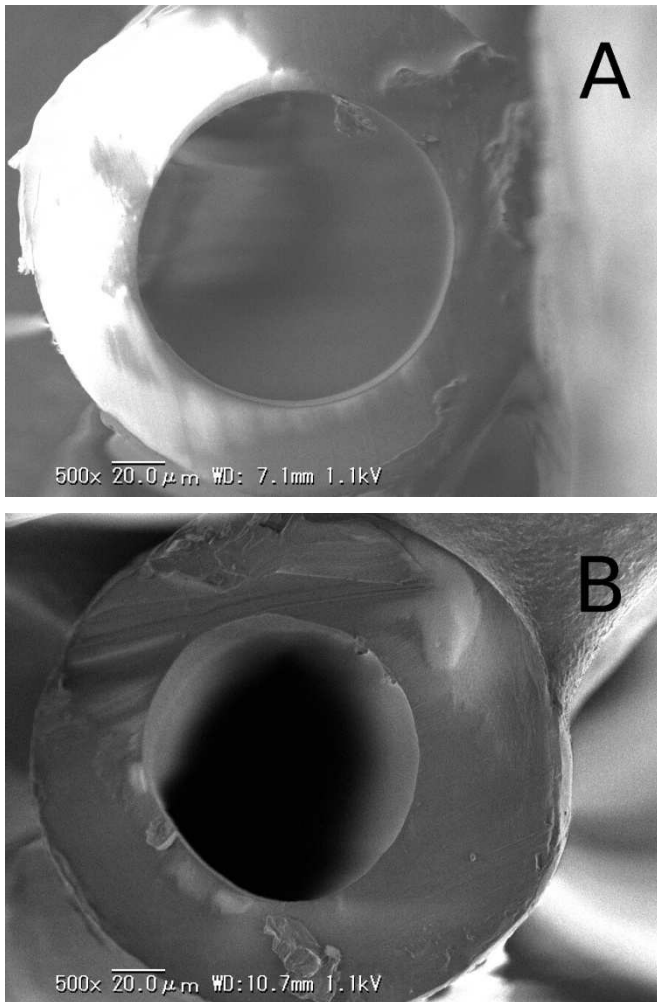


**FIGURE 1. (A) CAPILLARY A ,AVERAGE DIAMETER 114.5  $\mu\text{M}$  ,(B) CAPILLARY B,AVERAGE DIAMETER 100.1  $\mu\text{M}$**

Figure 2 shows the microcooler configuration for unloaded microcooler operation. A thermocouple was inserted into the evaporator of the microcooler at a distance of 1 mm from the capillary outlet. We have chosen a thermocouple diameter of 50  $\mu\text{m}$  to minimize heat in-leak through the thermocouple connection. The second microcooler configuration displayed in Figure 3 was used to measure cooling power. The end of the microcooler was covered by a metal casing encapsulating the evaporator. This metal casing is attached to an alumina block ( $\lambda = 30 \text{ W m}^{-1} \text{ K}^{-1}$ ) connected to a heater chip simulating the device being cooled. A predetermined heat input is introduced via the heater chip into the evaporator and the resulting evaporator temperature is measured by a resistance thermometer located on the heater chip. The operating temperature for a value of cooling power can thus be measured.

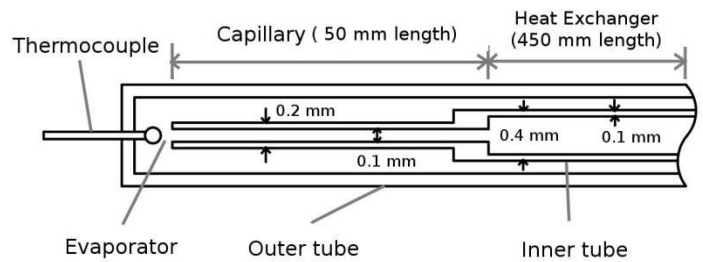


**FIGURE 2. MICROCOOLER CONFIGURATION FOR UNLOADED TRIALS**

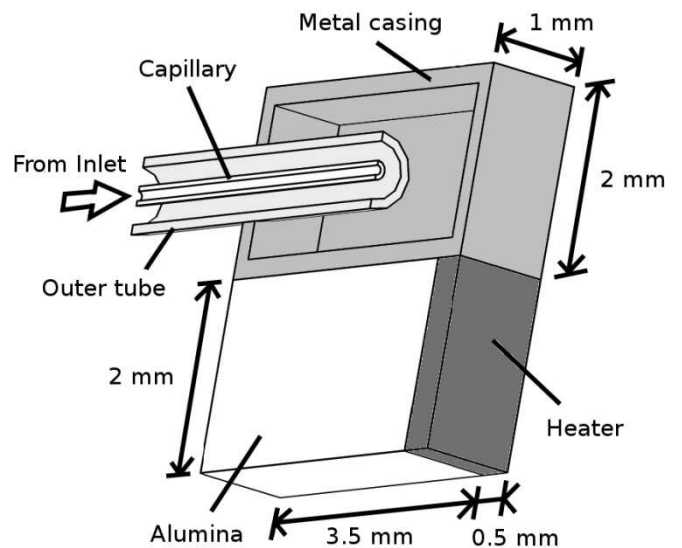


**FIGURE 3. MICROCOOLER CONFIGURATION FOR HEAT LOAD TRIALS**

Experiments were conducted using the setup shown in Figure 4. Inlet and outlet pressure and temperature were recorded in the manifold to which the microcooler was

connected. Mass flow rate was calculated by relating the gas density based on the outlet temperature and pressure to the volume flow rate measured at the outlet. The microcooler was positioned within a vacuum chamber to allow trials within vacuum conditions.

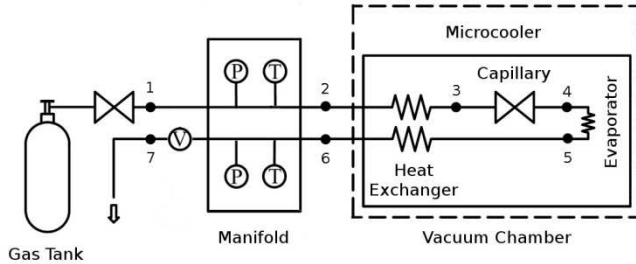


**FIGURE 4. APPARATUS SETUP**

## MASS FLOW RATE CALCULATION

In the microscale, gas flow cannot immediately be assumed to be a continuum due to rarefaction. The degree of rarefaction increases with the increase of the Knudsen number, which is the ratio of mean free path ( $\lambda$ ) to characteristic length ( $L$ ).

$$Kn = \frac{\lambda}{L} \quad (1)$$

At higher Knudsen numbers, the flow will feature increased rarefaction and its effects become more significant. In regards to this gas microflows can be classified into four categories: free molecular flow, transitional flow, slip flow, and continuum flow. Continuum flow is present at Knudsen numbers smaller than  $10^{-2}$ . In this study, the Knudsen numbers obtained were less than  $5 \cdot 10^{-4}$  therefore the flow can safely be assumed as continuum flow and thus Navier-Stokes based equations are applicable.

The inherent feature of the Joule-Thomson microcooler is the isenthalpic expansion of the coolant gas. In our device, this expansion is obtained using a capillary thus there will be a flow velocity limitation to the speed of sound due to choke. Using this flow velocity limit as a reference, it is possible to determine the mass flow rate of the coolant gas for a given inlet pressure.

The isenthalpic expansion is responsible for the cooling of the gas. Temperature and pressure will change thus also changing the thermophysical properties of the gas through the capillary. Since we rely on the speed of sound to determine mass flow rate, the properties of the gas must be continually calculated while it expands and cools in order to obtain a correct speed of sound at the correct capillary outlet temperature. To address this, we will use the gas equations of state incorporated with the PROPATH code[12] allowing continuous calculation of thermophysical properties. Another

issue is incompressibility which cannot be immediately assumed due to the sonic speed at the capillary outlet. Therefore, we divide the capillary into  $N_{cap}$  number of elements, each of  $dx_{cap}$  length. We determined  $dx_{cap}$  as such to ensure that the density change between each element was less than 0.5%. By doing this, incompressibility can be assumed within each element. Dividing the capillary into elements will also facilitate calculation of the change of thermophysical properties as the gas passes through the capillary. A value of 5000 ( $dx_{cap} = 5 \cdot 10^{-2}$  mm) was considered sufficient for the value of  $N_{cap}$ . The PROPATH code was supplemented by NIST data [13] where needed.

An initial mass flow rate can be assumed based on a given microcooler inlet pressure and temperature. Gas density at each element is determined by the pressure and temperature of the element. Once density is known, the gas flow velocity can be calculated. Beginning with the capillary inlet which is at a known temperature and pressure, the pressure downstream can be calculated according to the pressure drop governed by the Darcy-Weisbach equation. Inlet pressures above 0.5 MPa give Reynolds numbers above 3000, with values of  $Re > 7000$  at inlet pressures above 1.0 MPa. For microchannels, the transition range is between Reynolds numbers of 1800 and 2200[14, 15].

Thus, the gas flow is well within the turbulent region therefore we can calculate the friction factor from the Petukhov correlation :

$$f = (0.790 \ln Re - 1.64)^{-2} \quad (2)$$

Temperature of the coolant gas will decrease due to isenthalpic expansion. Incorporating this in the calculation is done by assuming constant enthalpy throughout the capillary. By using the reduced pressure for every element obtained from the pressure drop and the constant enthalpy, the temperature can be obtained using the PROPATH code.

As stated above, the resulting capillary exit velocity should be equal to the speed of sound. If the assumed mass flow rate does not achieve this, it is increased incrementally. The pressure and temperature for each element is then recalculated. The iteration continues until the specified mass flow rate results in sonic velocity at the capillary outlet.

## HEAT TRANSFER CALCULATION

Once the mass flow rate and the temperature distribution in the capillary have been established, it is possible to calculate the heat transfer of the heat exchanger. Temperature and heat transfer between the high pressure gas, inner tube wall and low pressure gas was calculated using an axisymmetric 2D finite difference code. This will allow for evaluation of performance reduction due to axial conduction.

Within the heat exchanger the gas flow velocity is much lower than the capillary therefore it can use a lower horizontal element number count  $N$  and still be applicable for the

incompressibility assumption. We have used 450 elements after verifying that a 300 element increase to 750 horizontal elements only results in a 0.8% and 1.0% change in predicted mass flow rate and temperature respectively.

Using inlet pressures below 1.7 MPa, the cold section annulus featured laminar flow. Shah and London [16] provide tabulated values of heat transfer coefficients for annuli which were applicable for this calculation. The Nusselt number determining the convective heat transfer coefficients for turbulent flow was calculated using the Gnielinski equation [17]:

$$Nu = \frac{\frac{f}{8} (Re_D - 1000) Pr}{1 + 12.7 \left(\frac{f}{8}\right)^{1/2} \left(Pr^{2/3} - 1\right)} \quad (3)$$

Temperature distribution within the low pressure and high pressure gas sections is first assumed with the high pressure gas temperature distribution being uniformly at room temperature while the low pressure gas section is assumed to be linear based on the room temperature and the previously calculated capillary outlet temperature. These values will be used in the 2D axisymmetric model of the wall temperature distribution (Figure 5).

Once the temperature distribution within the wall has been obtained from the finite difference calculation, the heat transfer to the low pressure gas and from the high pressure gas can be calculated. The enthalpy of the fluid in each gas element  $n$  is then:

$$h_{c,n-1} = h_{c,n} + \frac{Q_{h,n} + Q_{e,n} + Q_{rad,n}}{\dot{m}} \quad (4)$$

$$h_{h,n+1} = h_{h,n} - \frac{Q_{h,n}}{\dot{m}} \quad (5)$$

Where  $Q_h$  is the heat transfer rate from the hot section to the cold section. The heat in leak is represented by  $Q_e$  and  $Q_{rad}$  which are the convective and radiative heat in-leaks from the environment into the cold section of the heat exchanger respectively. Based on the study by Golzar et al [18], we can estimate an absorptivity of 0.6 for the PEEK outer tube of the microcooler. This value was used to predict the value of heat in-leak due to radiation effects  $Q_{rad}$ . The heat in-leak due to free convection on the outer tube wall  $Q_e$  is estimated using the Nusselt number from the free convection relation for cylinders presented by Churchill and Chu [19] in Equation 6.

$$Nu = \left\{ 0.60 + \frac{0.387 Ra^{1/6}}{\left[ 1 + \left( \frac{0.559}{Pr} \right)^{9/16} \right]^{8/27}} \right\}^2 \quad (6)$$

Where  $Ra$  and  $Pr$  are the Rayleigh number and Prandtl numbers for the surrounding air. The heat in-leak and heat transfer will give a new value of enthalpy for each element. By referencing this and the calculated pressure for each element, we obtain the temperature for each element.

This updated temperature distribution is the used to recalculate mass flow rate which will return a new temperature distribution. This iteration will continue until the convergence criterion is met:

$$\left| T_{h,out}^{(i)} - T_{h,out}^{(i-1)} \right| < 0.005 \text{ K} \quad (7)$$

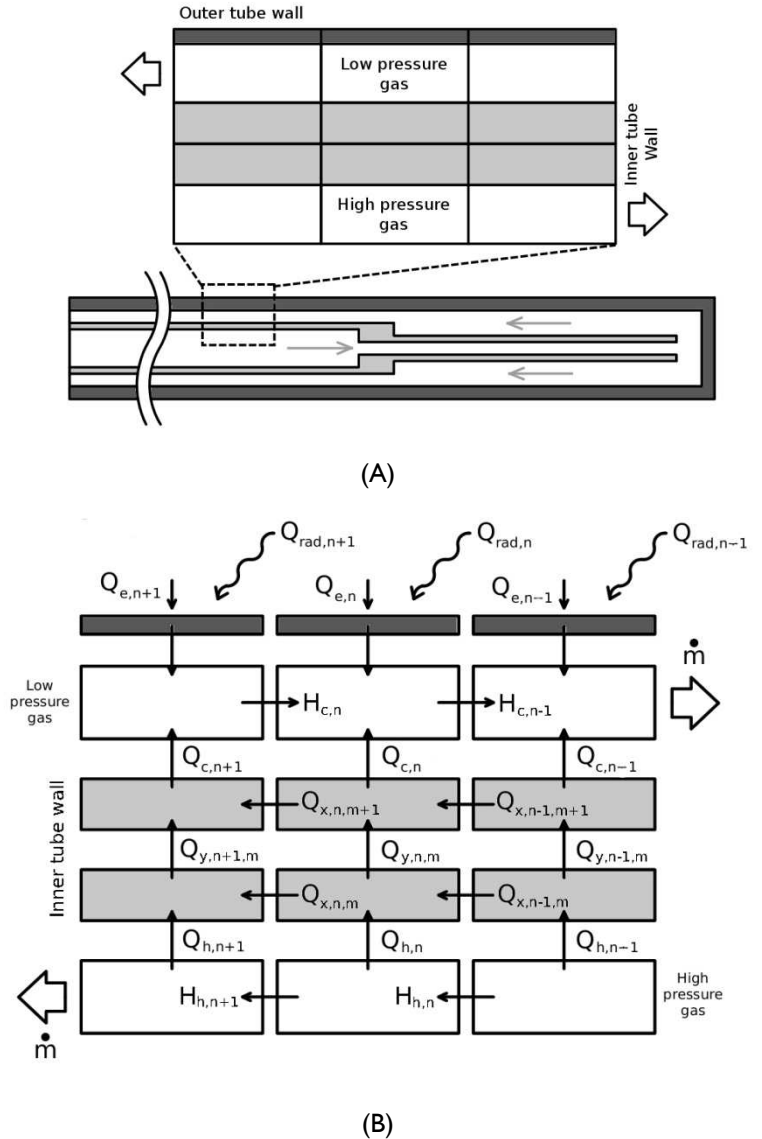


**FIGURE 5. DIAGRAM OF THEORETICAL MODEL. (A) SETUP OF ELEMENTS AND (B) BREAKDOWN OF HEAT TRANSFER PROCESSES**

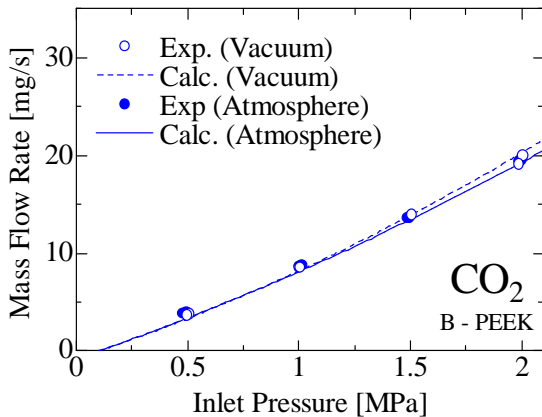
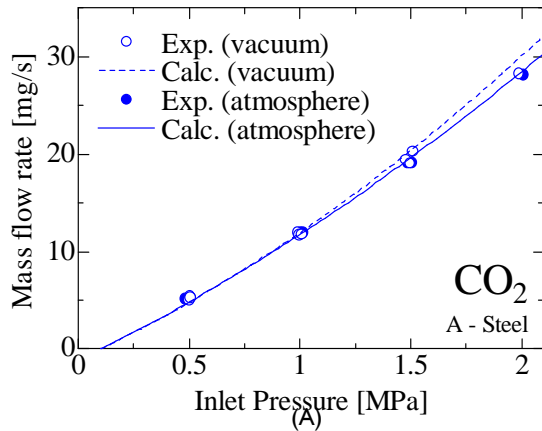


**FIGURE 6. UNLOADED THEORETICAL AND EXPERIMENTAL RESULTS OF MASS FLOW RATE FOR (A) MICROCOOLER A AND (B) MICROCOOLER B IN BOTH ATMOSPHERIC AND VACUUM ENVIRONMENTS**

## RESULTS AND DISCUSSION

Figure 6 shows a comparison between calculated and experimental values of mass flow rate for CO<sub>2</sub> trials conducted within a vacuum chamber. Mass flow rate calculations show a good degree of accuracy with under 10% deviation from experimental values. For microcooler A using capillary A, at 2.0 MPa inlet pressure, a predicted mass flow rate of 30.1 mg/s was obtained while experiments measured 28.3 mg/s. The smaller actual diameter of capillary B used in microcooler B resulted in a calculated mass flow rate of 20.79 mg/s at the same operating conditions compared to measured results of 19.4 mg/s.

Calculation and measurements for trials conducted in atmospheric conditions showing a similar degree of accuracy are also shown in Figure 6. At 2.0 MPa inlet pressure, Microcooler A had a 28.61 mg/s predicted mass flow rate. Experimental results were very close at 28.2 mg/s. Calculations

for Microcooler B pressure resulted in a 19.5 mg/s mass flow rate compared to a measured value of 19.4 mg/s.

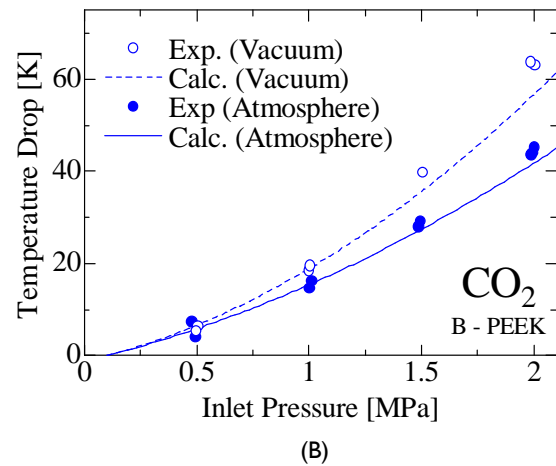
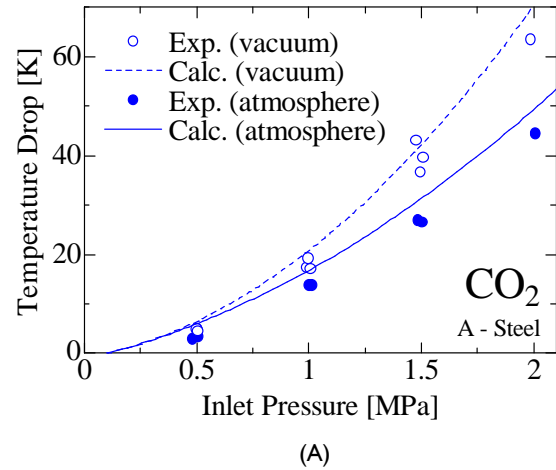


**FIGURE 7. UNLOADED THEORETICAL AND EXPERIMENTAL RESULTS OF TEMPERATURE DROP FOR (A) MICROCOOLER A AND (B) MICROCOOLER B IN BOTH ATMOSPHERIC AND VACUUM ENVIRONMENTS**

For incompressible laminar fluid flow, Hetsroni et al [14] conducted a study to verify the degree to which conventional macroscale theory could be used to estimate flow characteristics, finding that experimental results agree well with established theory. However, as stated by Morini et al [15] the inner diameter size of the microtube must be first verified properly to account for inaccuracy of manufacture. The significance of this can be observed from the mass flow rate of Microcooler A and B as the discrepancy between the nominal dimensions and the actual dimensions can cause notable differences.

Based on the good accuracy of the calculations of mass flow rate, we can see that for compressible flow in the turbulent regime, conventional correlations still hold well in predicting friction factor and pressure drop for microtubes as

long as dimensions are properly determined and assumption conditions such as the continuum assumption and the incompressibility assumption are valid.

Heat transfer calculations also displayed good accuracy from 1.0 MPa to 2.0 MPa for CO<sub>2</sub> as shown in Figure 7. Within vacuum conditions, at 2 MPa inlet pressure for microcooler A, a temperature drop of 70.2 K was predicted while the experiment obtained 63.5 K. Microcooler B had a predicted temperature drop of 57 K and a measure temperature drop of 63 K. In atmospheric conditions, a reduction in performance was observed due to the increased free convection. A predicted temperature drop of 49.7 K was obtained for Microcooler A while measured values gave 44.4 K. Predicted Microcooler B temperature drop was 43.9 K and measured temperature drop was 41.9 K.

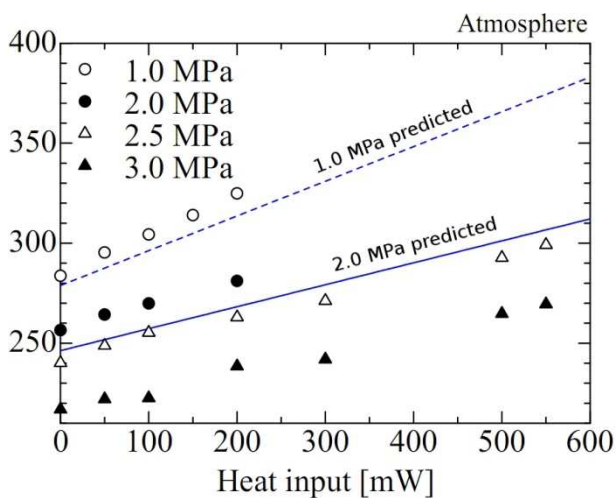


**FIGURE 8. THEORETICAL AND EXPERIMENTAL RESULTS HEAT LOAD TRIALS**

It should be noted that for CO<sub>2</sub> at 2.0 MPa inlet pressure, the mass flow rate will tend to become erratic and will decrease therefore reducing microcooler performance. We thus have a lower than predicted mass flow rate. This is due to the formation of dry ice within the capillary when the microcooler is performing normally. This dry ice will cause a blockage that will reduce mass flow rate. The performance will decrease to a level at around 50 K temperature drop where the dry ice will cease to persist thus returning performance to normal levels again. Eventually the cycle will repeat itself with normal operating levels followed by reduced performance and back to normal levels again and so on.

For microcooler A, the larger predicted temperature drop compared to measured temperature drop was expected. It is well known that heat in-leak is a source of inefficiency in Joule Thomson microcoolers[20]. While we have accounted for several sources, there remains heat in-leak sources unaccounted for such as the thermocouple connections therefore still resulting in a higher predicted temperature drop.

However, the results for Microcooler B show that measurements of temperature drop in fact exceed theoretical results. It should be remembered that we have employed PEEK as the inner tube material for Microcooler B. The inner tube is exposed to a high pressure coolant gas and the PEEK inner tube is a distensible material whereas Microcooler A uses a rigid steel material as the inner tube. The fact that the discrepancy is more pronounced at high pressures shows that it is most likely that distension and deformation of the inner tube dimensions is the cause. The mass flow rate is not influenced much by this as the mass flow rate is determined by the capillary diameter not the inner tube diameter.

A comparison of measured and predicted cooling powers for CO<sub>2</sub> is shown in Figure 8. We have mentioned above that the measurement configuration for cooling power is different from unloaded temperature measurement and therefore the degree of accuracy differs. The measurement of temperature and cooling power was done in the heater chip, much farther from the capillary outlet than in unloaded trials. In addition, the metal cover encasing the capillary outlet of the microcooler may account for additional heat in-leak. This has resulted in zero heat input evaporator temperature being approximately 5 K higher than unloaded trials when it should be the same.

Calculations predict the temperature at the capillary outlet, while the heat input configuration measured temperature at the heater chip. Thus, for all tested heat input magnitudes, the experiments with the heat input configuration have approximately a 7 K and 12 K deviance from calculated values for 1.0 MPa and 2.0 MPa inlet pressures respectively. However, the gradient of heat input to the predicted evaporator temperature is the same as the measurements. Putting into consideration the increased heat in-leak due to the metal casing and the different measurement locations, we can conclude that the operating temperature of the microcooler at a given heat input can be predicted with sufficient accuracy.

## CONCLUDING REMARKS

The model, employing conventional macroscale correlations, successfully combines the heat transfer within the heat exchanger with the isenthalpic expansion within the capillary. This has allowed the prediction of the wirtype Joule-Thomson microcooler performance with good accuracy using only the inlet gas pressure and temperature as input variables. It can be seen that conventional macroscale correlations hold well for the microscale conditions present.

By considering the coolant gas property change due to isenthalpic expansion and the choke near the capillary outlet, the mass flow rate was accurately determined within 10% of measured values. Temperature drop prediction was less accurate within 20% of measured values of the unloaded test likely due to a larger actual heat in-leak presence. In addition, for Microcooler B, there is also a possibility of PEEK inner tube deformation due to it being subjected to high gas pressures.

As can be seen from the heat load tests, for accurate results it is important that the simulation take into account actual measurement conditions and location. For the load tests, the fact that temperature measurement is conducted outside of the evaporator can result in a larger degree of discrepancy to calculated evaporator temperature. In addition, the presence of a metal casing encapsulating the evaporator may introduce increased heat in-leak.

Nevertheless, the results show that the model, using conventional macroscale correlations for turbulent microscale flow, can well represent the real performance of the microcooler. The method of calculation is therefore very applicable in the optimization of Joule-Thomson cooler designs and can be easily adapted for other gas species, microcooler materials and operating conditions.

## ACKNOWLEDGMENTS

This study was partially funded through the Grant-in-Aid for Scientific Research Fund in 2009-2010 (Project No. 21760159) by the Ministry of Education, Culture, Sports, Science and Technology, Japan.

## REFERENCES

- [1] Mazur, P., 1984, "Freezing of Living Cells : Mechanisms and Implications," *American Journal of Physiology : Cell Physiology*, 247, pp. C125-C142.
- [2] Cooper, I., 1964, "Cryobiology as Viewed by the Surgeon," *Cryobiology*, 51, pp. 44-51.
- [3] Smith, J. J., and Fraser, J., 1974, "An Estimation of Tissue Damage and Thermal History in the Cryolesion," *Cryobiology*, 11, pp. 139-147.
- [4] Rivoire, M. L., Voiglio, E. J., Kaemmerlen, P., Molina, G., Treilleux, I., Finzy, J., Delay, E., and Gory, F., 1996, "Hepatic Cryosurgery Precision : Evaluation of Ultrasonography, Thermometry, and Impedancemetry in a Pig Model," *Journal of Surgical Oncology*, 61, pp. 242-248.
- [5] Gage, A. A., and Baust, J., 1998, "Mechanisms of Tissue Injury in Cryosurgery," *Cryobiology*, 37, pp. 171-186.
- [6] Gage, A. A., Guest, K., Montes, M., Caruana, J. A., and Whalen, D. A., Jr., 1985, "Effect of Varying Freezing and Thawing Rates in Experimental Cryosurgery," *Cryobiology*, 22, pp. 175-182.
- [7] Lerou, P. P. M., Veenstra, T. T., Burger, J. F., Ter Brake, H. J. M., and Rogalla, H., 2005, "Optimization of Counterflow Heat Exchanger Geometry through Minimization of Entropy Generation," *Cryogenics* 45, pp. 659-669.
- [8] Derking, J. H., Brake, H. J. M. T., Sirbi, A., Linder, M., and Rogalla, H., 2009, "Optimization of the Working Fluid in the Joule Thomson Cold Stage," *Cryogenics*, 49, pp. 151-157.
- [9] Chou, F. C., Wu, S. M., and Pai, C. F., 1993, "Prediction of Final Temperature Following Joule-Thomson Expansion of Nitrogen Gas," *Cryogenics*, 33(9), pp. 857-862.
- [10] Maytal, B. Z., 1995, "Post-Isenthalpic Expansion Temperature," *Cryogenics*, 35(1), pp. 69-70.
- [11] Ng, K. C., Xue, H., and Wang, J. B., 2002, "Experimental and Numerical Study on a Miniature Joule-Thomson Cooler for Steady-State Characteristics," *International Journal of Heat and Fluid Flow*, 45, pp. 609-618.
- [12] Propath Group, 2001, PROPATH : A Program Package for Thermophysical Properties of Fluids, version 12.1
- [13] Lemmon, E. W., McLinden, M. O., and Friend, D. G., 2008, Nist Chemistry Webbook, Nist Standard Reference Database Number 69, National Institute of Standards and Technology, Gaithersburg MD, Thermophysical Properties of Fluid Systems.
- [14] Hetsroni, G., Mosyak, A., Pogrebnnyak, E., and Yarin, L. P., 2005, "Fluid flow in Micro-Channels," *International Journal of Heat and Mass Transfer*, 48, pp. 1982-1998.
- [15] Morini, G. L., Lorenzini, M., and Salvigni, S., 2006, "Friction Characteristics of Compressible Gas Flows in Microtubes," *Experimental Thermal and Fluid Science*, 30, pp. 733-744.
- [16] Shah, R. K., and London, A. L., 1978, *Supplement 1 to Advances in Heat Transfer*, Academic Press, New York.
- [17] Incropera, F. P., Dewitt, D. P., Bergman, T. L., and Lavine, A. S., 2007, *Fundamentals of Heat and Mass Transfer*, John Wiley & Sons, Hoboken, NJ.
- [18] Golzar, M., Beureuther, R., Brünig, H., Tändler, B., and Vogel, R., 2004, "Online Temperature Measurement and Simultaneous Diameter Estimation of Fibers by Thermography of the Spinline in the Melt Spinning Process," *Advances in Polymer Technology*, 23(3), pp. 176-185.
- [19] Churchill, S. W., and Chu, H. H. S., 1975, "Correlating Equations for Laminar and Turbulent Free Convection from a Horizontal Cylinder " *International Journal of Heat and Mass Transfer*, 18, pp. 1049-1053.
- [20] Gupta, P., and Atrey, M. D., 2000, "Performance Evaluation of Counter Flow Heat Exchangers Considering the Effect of Heat in Leak and Longitudinal Conduction for Low-Temperature Applications," *Cryogenics*, 40, pp. 469-474.